Colloidal assembly and active tuning of coupled plasmonic nanospheres

Zhiwei Li<sup>1</sup>, Wenshou Wang<sup>2</sup>, and Yadong Yin<sup>1,\*</sup>

<sup>1</sup>Department of Chemistry, University of California, Riverside, CA 92521, USA

<sup>2</sup>National Engineering Research Center for Colloidal Materials and School of Chemistry and

Chemical Engineering, Shandong University, Ji'Nan 250100, PR China

\*Correspondence: yadong.yin@ucr.edu (Y. Yin)

Abstract

Localized surface plasmon resonance (LSPR) originates from the collective oscillation of

conduction electrons when conductive nanoparticles are exposed to an electromagnetic field. It

generates remarkably enhanced electric fields surrounding the nanoparticles and leads to strong

extinction at the resonant wavelength. When plasmonic particles are in considerably close

proximity, plasmon coupling occurs because of the interacting resonance of the excited plasmon.

It enables the hybridization of the initial plasmon bands in the form of peak shift or reshaping of

local bands. Colloidal self-assembly approaches offer many opportunities for manipulating

particle arrangement, making it possible to actively tune the plasmon coupling in response to

external stimuli, which may promise important applications in many fields such as colorimetric

sensing and enhanced spectroscopic detection.

Keywords: LSPR; coupling; self-assembly; colorimetric sensors; SERS; enhanced fluorescence

### LSPR and plasmon coupling of nanoparticles

Plasmonic nanoparticles, particularly of noble metals, have broad applications because of their intriguing localized surface plasmon resonance (LSPR, see Glossary) [1, 2], which is determined by their chemical composition, size, shape, and surrounding dielectrics [3, 4]. The electron oscillation excited by light is localized on the particle surface, the so-called surface plasmon, and can regulate the propagation of light within the diffraction limit. When plasmonic nanoparticles self-assemble in close proximity, the surface plasmon of particles couple, resulting in a shift of the initial plasmon band [5, 6]. Depending on the morphology and size of the assembled structures, the plasmon coupling can be tuned to cover a broad range of spectra. Such remarkable spectral tuning holds significant potential for many light-involved applications [4, 7, 8], including colorimetric sensing [9-11], spectroscopic detection [12, 13], photocatalysis[14, 15], plasmon rulers [16-19], optical devices [20, 21], nanomedicine [22], and biosensing [23] (Figure 1). Among many methods, solution-phase self-assembly of plasmonic nanoparticles represents an efficient way for rapid creation and reversible modulation of plasmon coupling [24-28]. After more than two decades of effort, plasmon coupling can now be produced in various nanostructures using robust methods such as ligand-mediated assembly, field-guided assembly, orientation attachment, and fusion of nanocrystals [29-31].

Recently, there has been significant progress in preparing plasmonic assemblies with tunable coupling by solution-processed self-assembly. Since many reviews are available to provide a comprehensive introduction to LSPR and its applications (Figure 1) [1, 5, 12, 32-41], in this Opinion, we aim to focus our discussions on current research activities in the active tuning of the plasmon coupling by solution-processed self-assembly of nanospheres. As plasmon coupling is highly dependent on the spatial arrangement of the nanospheres within an assembly, we begin with an introduction to the assembly mechanisms which involve balancing entropic or other particular underlying interparticle forces, and then the assembly pathways which are analogous to polymerization reactions. Then, we summarize recent research efforts toward the design of responsive plasmonic assemblies for emerging applications in the fabrication of stimuli-responsive devices. Our discussions will focus on colorimetric sensing and spectroscopic

detection, two of the most actively explored applications in plasmonic materials. For interesting perspectives of other applications involving plasmon coupling, we invite the readers to refer to some comprehensive reviews [14, 36, 38, 42]. At the end of this review, we discuss the current major challenges that hinder the further exploration of new opportunities in this promising field.

# Colloidal self-assembly mechanism and pathways

Assembly mechanism: balancing dynamic forces for thermodynamic equilibrium

Plasmonic nanoparticles are conductive inorganic nanoparticles that are stabilized by a layer of capping ligands. The capping ligands, typically organic molecules also known as stabilizers or passivating ligands, can stabilize the colloidal nanoparticles from chemical or physical transformations. Previous studies have reached an agreement that, similar to the solvent interface of any chemical compounds in solution, there exists a solvation layer surrounding the colloidal particles due to interactions between the capping ligands and solvent molecules [43, 44]. This solvation layer provides electrostatic and/or steric repulsion to counter the attractive van der Waals (vdW) force [45].

The isotropic vdW force itself (or in combination with **entropic forces**) drives the formation of dense clusters or close-packed crystals, producing broadband absorption in the spectrum [46]. Specifically, in colloidal systems, entropic forces are the colloidal interactions caused by the osmotic pressure that arises from particle crowding. A typical example is the depletion force, which is usually responsible for driving the self-assembly of colloidal particles into 3D architectures. The exquisite control over the assembled structures, which affects the strength and quality of plasmon coupling, requires a counterforce. Typical counter forces include the long-range electrostatic repulsion or short-range steric repulsion, the latter stemming from overlapping solvation layers or the steric hindrance between capping ligands [26, 46, 47]. The dynamic balance between vdW attraction and sole or joint underlying repulsion can provide fine control over the assembly of plasmonic nanoparticles [48]. The classic definition of Coulomb electrostatic repulsion suggests that its strength depends on ionic concentration, pH, temperature, the dielectric constant of solvents, and charge density of the nanoparticles [25]. An

interesting property of the **electrical double layer** is its reconfiguration depending on structural geometry [49]. Consider a plasmonic oligomer formed by joining monomers (originally isolated nanoparticles) at the early assembly stage. Its solvation layer reconfigures to wrap the whole oligomer (Figure 2A), producing anisotropic electrostatic repulsion to its neighbors. The adjacent nanoparticles experience a stronger repulsive force when approaching the oligomer from its sides than ends, which leads to chain-like growth of the oligomer and excludes the formation of dense clusters. When monomers are depleted, the fusion of large chains becomes difficult and less selective [50], giving rise to a preferential assembly of branched chains. This phase behavior has been observed in pH-, salt-, and temperature-driven assembly processes [51-56]. Apparently, producing 1D ordered superstructures without branches or other defects requires strong anisotropic driving forces that can prevent the formation of possible isomers. Several reported strategies include the self-assembly of plasmonic nanoparticles in templates [57], the use of polymer shells to assist the 1D assembly of plasmonic particles [58], DNA-assisted self-assembly [59], metal complex-induced assembly [60], and self-assembly through specific molecular recognition [61].

The interaction of colloidal particles can be described by the classic Derjaguin-Landau-Verwey-Overbeek (DLVO) theory [62]. Dependent on the interparticle distance (r), the total interaction potential V(r) is a sum of electrostatic ( $V_{el}$ ), vdW ( $V_{vdW}$ ), and other contributing potentials (V'):  $V(r)=V_{el}+V_{vdW}+V'$ . DLVO theory relies on many assumptions to approximate colloidal interactions, which in turn set limitations to its use. For example, DLVO theory treats metallic cores as simply shaped spheres or less often ellipsoids with negligibly small capping ligands. It provides a considerably adequate description of particle behavior of sizes larger than ~50 nm but faces increasing difficulties as the particle size decreases due to the dynamic organic-inorganic interfaces and highly faceted, imperfect structures [63]. Fortunately, a series of important new concepts have recently been proposed to solve the problem of **nonadditivity** at the nanoscale, with molecular simulation methods rising as emerging tools to analyze the correlated forces between nanoparticles [64]. In summary, when the repulsive force between plasmonic nanospheres is weak, they usually self-assemble into dense clusters or crystals. Enhancing the

repulsive interaction can produce branched chains. The assembly kinetics is a key factor but not decisive to determine the chain architectures.

Assembly pathways: step-growth versus chain-growth polymerization

In the past decade, experimental results have revealed that the self-assembly of plasmonic nanoparticles somewhat resembles a polymerization process, with growth pathways and polydisperse intermediates similar in many ways to those involved in the formation of organic polymers [65-71]. Treating colloidal nanoparticles as monomers in polymerization, one can define the colloidal chain size in terms of particle numbers. The degree of accuracy within which plasmonic assemblies can be predicted is similar to that well-established in synthetic polymers. It enables defining the average number of particles in the plasmonic chains and designing complex assembly structures for desirable functions through branching and jointing of plasmonic monomers or oligomers.

Because plasmonic particles tend to aggregate in specific chemical environments, their selfassembly normally occurs in a manner similar to step-growth polymerization [65, 67, 72]. As illustrated in the right panel of Figure 2B, monomers (individual nanoparticles) first assemble into oligomers (short chains of a few nanoparticles), which serve as subunits and can be further linked to form large chains [73]. The chain size increases slowly initially but more dramatically in the later stage of the assembly process [65]. In other cases, the assembly favors the chain-growth pathway (left panel in Figure 2B), where long chains are formed at a low rate of particle addition [58]. Specifically, individual nanoparticles are gradually added to the chains to support the chain growth. Thus, monomer concentration and reactivity remain comparatively higher than that in the step-growth mode. This understanding partially explains why linear or branched chains are formed in particular assembly conditions. For example, branched chains containing highly crosslinked short chains are unlikely to be formed through the chain-growth pathway. During stepgrowth, plasmonic oligomers of high concentration have similar anisotropic interactions, thus still favor branching under kinetic control. More specifically, the side bonding sites on intermediate oligomers are much more than the ends, leading to a kinetically favored branching effect. According to previous reports, both pathways can produce linear chains [58, 67, 74]. Several detailed investigations have recognized that the formation of linear chains requires delicate control over the driving force [75].

## **Hybridization of plasmon modes**

Proposed by Halas and Nordlander, plasmon hybridization is an analytical method to describe the coupling between plasmonic nanoparticles [76-78]. Considering a plasmonic dimer that is excited along the interparticle axis, the plasmon mode is hybridized in a way similar to the  $\sigma$ covalent bond in the hybridization of atomic orbitals (Box 1). The initial dipole mode is hybridized into two plasmon modes: the low-energy "bonding" mode (σ) and the high-energy "antibonding" mode ( $\sigma^*$ ) [79]. The "bonding" mode is also referred to as the bright mode, which is redshifted from the original band position (inset in Figure 2C). When the plasmonic dimer is excited laterally, the dipole couples resembling a  $\pi$  bond in organic molecules. Because the dipoles are anti-aligned in  $\sigma^{*}$  and  $\pi$  modes, the zero net moment does not induce measurable peaks in the extinction spectrum. Therefore, only  $\pi^*$  coupling mode is observable in lateral excitation but with blueshifts due to the "antibonding" manner of the two dipoles. Several close investigations on the optical properties of metal dimers that are carefully prepared by nanomanipulation or lithographic techniques have confirmed the peak shift in the  $\sigma$  and  $\pi^*$  coupling modes [19, 79]. Figure 2C indicates the peak position of the o mode of a plasmonic chain. Both the wavelength and intensity of the coupling peak increase as the interparticle gap decreases. The calculated position of the coupling peak has a semi-exponential dependence on the gap size. Several quantitative studies have also suggested an empirical exponential equation:  $\Delta\lambda/\lambda_0 = a \cdot e^{-x/\tau}$ .  $\Delta\lambda/\lambda_0$  is the normalized peak shift and x is the reduced gap size (i.e., gap size over particle diameter). Due to the enhanced coupling effect, the peak shift of plasmonic chains increases with increasing the particle number (Figure 2C). For anisotropic plasmonic assemblies, the coupling strength and peak intensity of each mode are dependent on the chain orientation relative to light polarization. A few studies suggest that the excitation of  $\sigma$  coupling mode can be described by  $\cos^2\Theta$ , where  $\Theta$  is the angle between chain orientation and polarization (Figure 2D) [80, 81]. The electric field localized in the gap is sensitive to the gap size and chain orientation and can be enhanced by hundreds of times (Figure 2E). Interestingly, the LSPR of plasmonic chains is two orders of magnitude stronger than

that of single plasmonic particles. In a general sense, the LSPR at the resonant frequency reconfigures to a coupled resonance at the coupling frequency through energy hybridization (Figure 2F). This process induces color changes due to the peak shift of plasmon bands, which represents a promising approach to colorimetric sensors. When fluorescent or Raman molecules are near the surface of plasmonic assemblies, their emission or scattering can be remarkably enhanced due to the energy transfer occurring at their excitation frequency. The large enhancement of local field strength in plasmonic chains is ideal for enhanced spectroscopy as it will promote the energy transfer between the plasmonic assemblies and fluorescent molecules (Figure 2F).

# Creation of plasmon coupling through colloidal assembly

In solution-processed assembly, plasmonic nanoparticles ranging from 5 to 50 nm are ideal for preparing responsive optical nanostructures for a few reasons. First, such large particles have sharp plasmon bands at short wavelengths, which facilitates the tuning of their plasmonic peak over a wide spectral range during self-assembly. Particles out of this size range have low plasmonic activity (size < 5 nm) [82] or multiple scattering-dominated plasmon bands in the visible range (size > 50 nm) [83, 84]. Second, the entropic force of nanoparticles in this size range is comparable to their electrostatic forces, which provides easy control over their assembly behaviors [85, 86]. For self-assembly using specific interactions of DNA or metal complex, the size of plasmonic nanoparticles can be larger due to these strong driving forces [87]. In addition, researchers have developed a number of methods to prepare particles of tens of nanometers. Their high crystallinity, narrow size distribution, and tunable surface functionalization are highly desired in studying the fundamental aspects of plasmonic coupling and providing well-defined optical properties for many practical applications. Producing considerably larger metal nanoparticles is limited to a few methods. Additionally, large particles usually have a rough surface and large morphological variation [83, 84]. For small particles, their faceted surface and high surface energy make them unstable. The overlap between crystal nucleation and growth is another challenge for synthesizing monodisperse plasmonic particles of a few nanometers [63].

Early research focused on the self-assembly of Au nanospheres into 2D and 3D assemblies [88-90]. After being exploited for decades, the self-assembly of plasmonic particles has achieved elegant control over their spatial configuration [27, 91-93]. In a typical strategy, increasing ionic strength can effectively screen electrostatic interactions between charged nanoparticles. From the energy perspective, increasing ionic strength can lower the electrostatic potential  $(V_{el})$  in the DLVO theory, thus possibly creating a global minimum in the interparticle energy profile and a stable assembled state [47]. Therefore, adding a salt solution to a colloidal dispersion of Au nanoparticles produces highly cross-linked 2D chains (Figure 3A, B) [91]. As ionic concentration increases, plasmonic particles self-assemble into long chains, resulting in a gradual redshift of the coupling peak (Figure 3C). That is because adding more salts will create a higher tendency for nanoparticles to assemble due to the further decrease in  $V_{el}$  and increase in entropic forces in high ionic strength. When a citrate-based capping ligand is used, its binding to the Au surface is relatively weak so the assembly is irreversible due to the dynamic nature of the organic-inorganic interaction, which allows the ligand to dissociate from the nanoparticle surface. Due to the dissociation, the Vel between particles cannot recover the initial value before assembly and therefore the assembled structures remain stable although the ionic strength is reduced by adding water. A stronger capping ligand can ensure a stable and sufficient interparticle repulsion so that the assembly can be tuned reversibly by adjusting the ionic strength of the solution which controls the Debye screening and therefore particle interaction [94]. More interestingly, the reversible plasmonic assembly can also be achieved by controlling the temperature of the solution, which, according to DLVO theory, modulates the electrostatic interaction [46, 95, 96]. As no extra chemicals are involved, the assembly of Au nanoparticles and their plasmon coupling can be reversibly modulated without any change to the chemical composition of the system [27].

From an application perspective, an extension of the assembly strategy to Ag is highly desirable since Ag has the appropriate electron structure and dielectric function to support stronger LSPR than does Au [35, 97, 98]. As Ag is prone to oxidize in the presence of a strong capping ligand, a polymeric ligand with multiple weak binding groups is required to ensure sufficient overall binding strength. In this case, a 'limited ligand protection' strategy is used to induce the assembly of nanoparticles in a controllable manner (Figure 3D) [99, 100], producing a broad coupling band

that continuously redshifts as the assembly proceeds (Figure 3E) [101]. Reversible tuning of the plasmonic coupling can be realized by disassembling/assembling the nanoparticles by controlling the charge dissociation of the capping ligands. For example, when polyacrylic acid (PAA) is used as the capping ligand, increasing the pH of the solution promotes deprotonation of the carboxyl groups and creates more surface charges, inducing nanoparticle disassembly and resulting in blueshift of the plasmonic band [66]. The subsequent decrease in the pH of the solution leads to the re-assembly of the nanoparticles and the redshift of the spectrum.

The chain-growth scheme is expected to produce long linear chains of one-particle width. This phase behavior was discovered in the self-assembly of block copolymer-capped Au nanoparticles, which involves first the particle self-assembly and then reconfiguration of the copolymer shell (Figure 3F) [41]. As activated by the hydrophobic interaction and vdW attraction, Au oligomers formed because of reduced electrostatic repulsion. As shown in Figure 3G, these structures are metastable due to the high interfacial energy of the separately coiled copolymer layer. As a result, the copolymer shell starts to reconfigure into a conformal, cylindrical coating at high temperature. The hydrophilic and hydrophobic domains gradually separate to form cylindrical micelles (represented by light domains around chains in Figure 3G) [102, 103]. The cylindrical micelles further exert weak repulsion to Au particles that are approaching from the chain end due to the relatively low copolymer density at the curved end, which eventually induces the end-on attachment [104-106]. The thermodynamic stability of copolymer micelles, in addition to the electrostatic repulsion, further impedes branch formation [58]. Their joint effects are believed to exert more dramatic force anisotropy between end- and side-attachment, which demonstrates the dominant role of driving forces in manipulating chain architectures.

### Responsive plasmon coupling for colorimetric sensing and spectroscopic detection

Responsive plasmon coupling provides an ideal platform for many colorimetric applications, including dynamic color display, encryption, camouflage, sensing, and anticounterfeiting [107-111]. It produces a dynamic shift of the coupling peak and thus perceptible color changes in response to external stimuli, such as heat, electric fields, magnetic fields, light, chemicals, and mechanical perturbations [4]. When Raman or fluorescent molecules are coupled to responsive

plasmonic assemblies, their SERS or emission can also be actively tuned by external stimuli, which lays the foundation for many enhanced spectroscopic detection techniques. Compared with other modern sensors, like electrochemical or capacitive sensors that generate electric responses, the plasmonic coupling-based detection techniques are inherently advantageous in many aspects: i) it is much simpler in terms of both the sensor fabrication and the detection procedure; ii) it provides comparable sensitivity in a much lower cost; iii) it is compatible with various fabrication and synthesis processes, such as lithography and coating processes, and can thus be incorporated into many functional materials for real-time detections in solution, solid-state, and biological environments. In this section, we will discuss responsive plasmonic coupling for colorimetric sensing and spectroscopic detection.

Figure 4A illustrates the working principle of a plasmonic pressure sensor, which is based on the stress-induced decoupling of Au nanospheres [10]. The colorimetric film is prepared by embedding Au chains that are assembled through salt-initiated self-assembly into polymer matrices. Under external pressure, the polymer matrices expand and the distance between Au nanospheres increases accordingly, leading to a gradual blueshift of the plasmon band (Figure 4B). Meanwhile, the film color changes from blue to ruby red (Figure 4C), which indicates a transition from the coupling mode of Au chains to the simple resonance band of isolated Au nanospheres. Although solid-state sensors are often more desirable, achieving rapid and reversible plasmonic responses to pH or solvent composition is more challenging when nanoparticles are not dispersed in solution, largely because of the lack of an efficient way to control the surface changes of plasmonic particles and the interparticle spacing in a solid film. Recently, a novel approach to a solid colorimetric plasmonic sensor is introduced by coupling the humidity-sensitive salt hydrolysis with the spacing changes between PAA-caped Ag nanoparticles [112]. In this work, sodium borate (Na<sub>2</sub>B<sub>4</sub>O<sub>7</sub>) releases OH<sup>-</sup> when it hydrolyzes in contact with water (Figure 5A). The released OH- deprotonates carboxyl groups of PAA on Ag nanospheres and further weakens the plasmon coupling due to the increases in the surface charges and eventually the interparticle separation. When water evaporates, the hydrolysis reaction reverses, which protonates the surface PAA and recovers the plasmon coupling. These reversible processes create rapid color changes in the solid film in response to a trace amount of water, such as the

vapor generated by fingertips and breath. If Ag nanospheres were fused by Ostwald ripening under UV light, the jointed particles exhibit a negligible peak shift upon exposure to water vapor. Therefore, an image can be created with potential applications in information encryption and touchless sensing (Figure 5B).

Another promising application of plasmon coupling is enhanced spectroscopy. This advanced technique is based on the energy transfer between the localized electromagnetic field and coupled Raman or fluorescent molecules. Early enhanced spectroscopy uses the LSPR of single nanoparticles. It relies on particles with sharp features for high surface-enhanced Raman spectroscopy (SERS) activity but is also limited by the challenges in synthesizing highly faceted and anisotropically shaped plasmonic crystals. Alternatively, plasmon coupling has been developed for next-generation SERS with high sensitivity (Figure 6A). The electromagnetic theory has been established to explain the enhanced Raman scattering of molecules in SERS (Figure 6B). The excitation and emission of Raman molecules with small chemical shifts are enhanced in sequence at the resonant frequency of plasmonic particles, resulting in an overall enhancement factor of  $E^4$  (Box 2), where E is the local strength of electric field [113]. Due to the separated excitation and emission in the enhanced fluorescence, it can only benefit from the local field enhancement at the incident frequency and therefore has a theoretical enhancement factor of  $E^{2}$  [39]. With this approximation, it is possible to predict the enhancement factor of particular plasmonic assemblies. As an example (Figure 6C), the Raman scattering can be theoretically enhanced by ten orders of magnitude by a linear Au chain. A further comparison indicates that enhancement in plasmon coupling is two to four orders of magnitude greater than that in isolated nanoparticles. Another unique character is the gap-dependent enhancement occurring at the resonant frequency, which underpins the theoretical possibilities to actively tune SERS. Several common practices use responsive interactions between nanoparticles or transformations of functional molecules that are modified on plasmonic particles. These strategies include conformational changes of pH-responsive copolymers [114], specific interactions between biological molecules [13, 115], hydrogen bonding [116], and electrostatic interactions [39]. For example, active SERS was reported on Au nanoparticles capped by pH-responsive copolymers [114]. Considering a carboxylic acid-terminated copolymer, it has an expanded conformation at

pH > 4. The strong steric and electrostatic forces prevented Au particles from assembling, resulting in low SERS activity (Figure 6D). At pH < 4, the polymer has a condensed conformation, which guided the self-assembly of Au nanoparticles into small clusters. These sequences of events could reversibly tune the SERS activities of the carefully prepared system in response to pH changes. Similarly, a fluorescent sensor could be developed by assembling plasmonic nanoparticles through the sequence-specific interactions between DNA. A fluorescence probe, Cyanine 5, was first linked to the DNA, whose fluorescence was quenched by the proximal plasmonic particles [117]. When the plasmonic Au particles were assembled through the DNA recognition, the fluorescence was enhanced with tunable enhancement factor in response to the change of the target DNA concentration. Plasmonic particles with Ag-rich surfaces and large sizes have high enhancement effects. Incorporating plasmonic nanoparticles into responsive substrates, like microgels or polymer matrix, is another effective way to achieve active plasmonic coupling [118]. When the Raman or fluorescent molecules are doped into the substrates, their enhanced scattering or fluorescence can be simultaneously tuned. This strategy takes advantage of many responsive polymers to dynamically control the separation between guest plasmonic particles and the energy transfer between the particles and the molecules. Poly(Nisopropylacrylamide) (PNIPAM), for example, can reversibly reconfigure from a hydrophilic swollen state to a hydrophobic collapsed state when the temperature increases above the lower critical solution temperature (~ 32°C) [119]. When Ag nanoparticles were formed in the PNIPAM microgels by in situ reduction, the fluorescence of doped chromophores can be tuned by changing the temperature [120]. This method provides similar sensitivity while it does not need sophisticated surface functionalization for balancing the interacting forces.

### **Concluding remarks**

The close morphological and kinetic similarities between plasmonic self-assembly and polymer science provide an analytical route to understanding and predicting the phase behaviors of plasmonic nanoparticle assembly. In a more general sense, the description of chain formation in colloidal self-assembly is still far from the scientific way as the synthetic polymer is documented. To exploit natural laws underlying the qualitative phenomena and general mechanism

summarized here, it is essential to analyze in detail the interacting forces. In addition to the spectroscopic techniques, synchrotron-based *in situ* characterization of chain growth and experiment-focused multiscale computation should be additional tools in studying plasmonic assemblies. From a practical perspective, developing reliable methods to assemble anisotropic plasmonic nanostructures into controllable configurations remains challenging although it is of particular interest in applications such as metamaterials, Fano resonance, and advanced optical devices (see Outstanding Questions) [121]. Overcoming these challenges will provide clear routes to interesting optical properties based on the unique coupling effects between plasmonic nanoparticles and enable the design of responsive systems to various external stimuli on demand.

# **Acknowledgments**

The research discussed in this article was supported at different stages by the U.S. National Science Foundation (CHE-1308587 and CHE-1808788).

# **Box 1.** Plasmon coupling in plasmonic assemblies.

The coupling strength of plasmonic chains is determined by interparticle separation, number of particles, and the orientation of chains. Under excitation, the harmonic oscillation of conductive electrons in metal nanospheres is described by the multipolar polarizability

$$\alpha_l = 3V \frac{l(\varepsilon - \varepsilon_m)\varepsilon_m}{l\varepsilon + (l+1)\varepsilon_m}$$
 [I]

where V is the volume of the nanoparticles;  $\varepsilon$  and  $\varepsilon_m$  the permittivities of particles and surroundings, respectively, and I the orbital moment number (1 for a dipole). The resonance occurs when  $\varepsilon$  is equal to  $-(I+1)\varepsilon_m/I$ . The extinction ( $\sigma_{\rm ext}$ ) and scattering cross-section ( $\sigma_{\rm sca}$ ) of particles can be calculated by the following equations

$$\sigma_{ext} = \sigma_{abs} + \sigma_{sca} = \frac{2\pi}{\lambda \sqrt{\varepsilon_m}} Im(\alpha_1)$$
 [II]

$$\sigma_{sca} = \frac{8\pi^3}{3\lambda^4} |\alpha_1|^2 \tag{III}$$

In interacting plasmonic dimers, the resonant frequency of coupling modes can be predicted by

$$\omega = \frac{\omega_P}{\sqrt{2 + \varepsilon_b}} \sqrt{\frac{1 + g}{1 + \eta g}} - \frac{i\tau^{-1}}{2}, \eta = \frac{\varepsilon_b - 1}{\varepsilon_b + 2}$$
 [IV]

given the values of g for different coupling modes in Figure IA. The  $\hbar\omega_P$  is equal to 9 eV; the damping rate,  $\hbar\tau^{-1}$ , is equal to 0.05 eV, and  $\epsilon_b$  is the background polarization of Au particles with a value of 9. The classic paper by Liz-Marzán and Abajo introduced these concepts for modeling the optical properties of Au particles [122].

Considering a linear plasmonic chain, its orientational state is described as a ket,  $|\Theta\rangle$  (Figure IB). Based on the bra-ket notation, its excitation state of the two  $\sigma$  modes is interpreted as a polarization operator,  $P=|y\rangle\langle y|$ , operating on the state function

$$C=P|\theta>=|y>< y|(\sin\theta|x>+\cos\theta|y>)=\sin\theta|y>< y|x>+\cos\theta|y>< y|y>=\cos\theta|y> \qquad [V]$$

The ket describes the direction of coupling and  $\cos\Theta$  is the excitation coefficient. The expectation value of the state function is a description of the coupling strength:

 $E=<\Theta \mid P\mid\Theta>=<\Theta \mid (\cos\Theta \mid y>)=(\sin\Theta < x\mid +\cos\Theta < y\mid )\cos\Theta \mid y>=\sin\Theta \cos\Theta < x\mid y>+\cos^2\Theta < y\mid y>=\cos^2\Theta \quad [VI]$ 

The coupling strength of the  $\sigma$  modes is proportional to  $\cos^2\theta$ , and the coupling strength of the  $\pi^*$  modes is similarly proportional to  $\sin^2\theta$ .

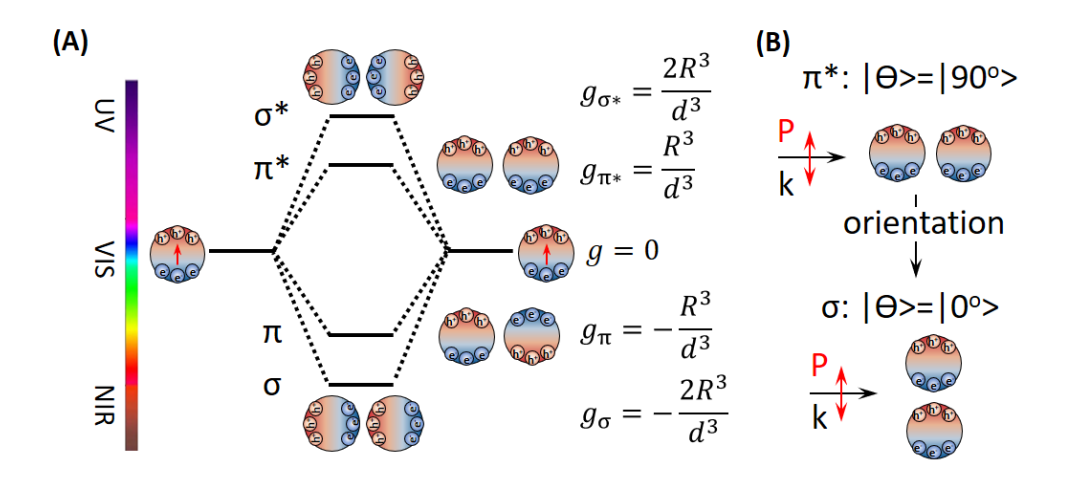


**Figure I.** (A) Energy hybridization in plasmonic dimers. Adapted with permission from [122]. (B) The excitation of the two bright coupling modes:  $\pi^*$  and  $\sigma$  at chain orientation of  $|90^\circ\rangle$  and  $|0^\circ\rangle$ , respectively. The wave vector and polarization of incident light are denoted as k and P, respectively.

# **Box 2.** Energy transfer in plasmon coupling for enhanced spectroscopy.

Enhanced spectroscopy, including plasmon-enhanced fluorescence and SERS, uses the LSPR of plasmonic nanostructures to enhance the emission or scattering of organic molecules. The enhanced excitation first happens at the resonant frequency ( $\omega_0$ ) of plasmonic particles, where their LSPR transforms the far field to the near field to enhance the excitation of SERS [123]. The first enhancement factor ( $G_1$ ) equals  $[E_{loc}(\omega_0)/E_0(\omega_0)]^2$ . At the Raman scattering frequency ( $\omega_R$ ), the enhanced emission is due to the coupling between the induced dipole of Raman molecules and the enhanced field of particles at  $\omega_R$ . The second enhancement factor ( $G_2$ ) is proportional to the square of the local electric field at  $\omega_R$ .

In Raman molecules with low-frequency vibrational modes and small chemical shifts, the  $E_{loc}$  of plasmonic particles and the enhancement factor at the two frequencies are comparable [113]. Therefore, the enhancement factor (G) can be estimated by the fourth power of the local electric field

$$G = G_1 \times G_2 = \frac{|E_{loc}(\omega_0)|^2}{|E_0(\omega_0)|^2} \times \frac{|E_{loc}(\omega_R)|^2}{|E_0(\omega_R)|^2} \approx \frac{|E_{loc}(\omega_0)|^4}{|E_0(\omega_0)|^4}$$
[VII]

For fluorescent molecules with a large shift between excitation and emission, the plasmon-enhanced fluorescence can only benefit from the enhancement at the resonant frequency with an estimated factor of  $[E_{loc}(\omega_0)/E_0(\omega_0)]^2$ .

#### References

- [1] Jiang, N. *et al.* (2017) Active plasmonics: principles, structures, and applications. *Chem. Rev.* 118, 3054-3099
- [2] Comin, A.and Manna, L. (2014) New materials for tunable plasmonic colloidal nanocrystals. *Chem. Soc. Rev.* 43, 3957-3975
- [3] Lu, X. et al. (2009) Chemical synthesis of novel plasmonic nanoparticles. *Annu. Rev. Phys. Chem.* 60, 167-192
- [4] Li, Z.and Yin, Y. (2019) Stimuli Responsive Optical Nanomaterials. Adv. Mater. 31, 1807061
- [5] Jain, P. K.and El-Sayed, M. A. (2010) Plasmonic coupling in noble metal nanostructures. *Chem. Phys. Lett.* 487, 153-164
- [6] Su, K.-H. *et al.* (2003) Interparticle coupling effects on plasmon resonances of nanogold particles. *Nano Lett.* 3, 1087-1090
- [7] Li, Z. et al. (2014) Magnetic targeting enhanced theranostic strategy based on multimodal imaging for selective ablation of cancer. Adv. Funct. Mater. 24, 2312-2321
- [8] Funston, A. M. et al. (2009) Plasmon coupling of gold nanorods at short distances and in different geometries. *Nano Lett.* 9, 1651-1658
- [9] Acimovic, S. S. et al. (2009) Plasmon near-field coupling in metal dimers as a step toward single-molecule sensing. ACS nano 3, 1231-1237
- [10] Han, X. et al. (2014) Colorimetric stress memory sensor based on disassembly of gold nanoparticle chains. *Nano Lett.* 14, 2466-2470
- [11] Stewart, M. E. et al. (2008) Nanostructured plasmonic sensors. Chem. Rev. 108, 494-521
- [12] Guerrini, L.and Graham, D. (2012) Molecularly-mediated assemblies of plasmonic nanoparticles for Surface-Enhanced Raman Spectroscopy applications. *Chem. Soc. Rev.* 41, 7085-7107
- [13] Qian, X. et al. (2008) Surface-enhanced Raman nanoparticle beacons based on bioconjugated gold nanocrystals and long range plasmonic coupling. J. Am. Chem. Soc. 130, 14934-14935
- [14] Brongersma, M. L. *et al.* (2015) Plasmon-induced hot carrier science and technology. *Nat. Nanotechnol.* 10, 25
- [15] Wang, H. et al. (2012) Au/TiO2/Au as a plasmonic coupling photocatalyst. J. Phys. Chem. C 116, 6490-6494
- [16] Teperik, T. V. *et al.* (2013) Robust subnanometric plasmon ruler by rescaling of the nonlocal optical response. *Phys. Rev. Lett.* 110, 263901
- [17] Liu, N. et al. (2011) Three-dimensional plasmon rulers. Science 332, 1407-1410
- [18] Sönnichsen, C. *et al.* (2005) A molecular ruler based on plasmon coupling of single gold and silver nanoparticles. *Nat. Biotechnol.* 23, 741-745
- [19] Jain, P. K. *et al.* (2007) On the universal scaling behavior of the distance decay of plasmon coupling in metal nanoparticle pairs: a plasmon ruler equation. *Nano Lett.* 7, 2080-2088
- [20] Wong, Z. J. *et al.* (2017) Optical and acoustic metamaterials: superlens, negative refractive index and invisibility cloak. *J. Opt.* 19, 084007
- [21] Kawata, S. *et al.* (2009) Plasmonics for near-field nano-imaging and superlensing. *Nature Photon.* 3, 388
- [22] Huang, P. et al. (2013) Biodegradable gold nanovesicles with an ultrastrong plasmonic coupling effect for photoacoustic imaging and photothermal therapy. *Angew. Chem. Int. Ed.* 52, 13958-13964
- [23] Wang, H. N.and Vo Dinh, T. (2011) Plasmonic coupling interference (PCI) nanoprobes for nucleic acid detection. *Small* 7, 3067-3074
- [24] Hsu, S.-W. *et al.* (2018) Colloidal plasmonic nanocomposites: from fabrication to optical function. *Chem. Rev.* 118, 3100-3120

- [25] Li, Z. et al. (2019) Smart Materials by Nanoscale Magnetic Assembly. Adv. Funct. Mater. 1903467
- [26] Liu, Q. et al. (2018) Optical tuning by the self-assembly and disassembly of chain-like plasmonic superstructures. *Natl. Sci. Rev.* 5, 128-130
- [27] Liu, Y. et al. (2012) Thermoresponsive assembly of charged gold nanoparticles and their reversible tuning of plasmon coupling. *Angew. Chem. Int. Ed.* 51, 6373-6377
- [28] Boltasseva, A. (2009) Plasmonic components fabrication via nanoimprint. *J. Opt. A: Pure Appl. Opt.* 11, 114001
- [29] Ribeiro, C. *et al.* (2006) Oriented attachment mechanism in anisotropic nanocrystals: A "polymerization" approach. *ChemPhysChem* 7, 664-670
- [30] Liang, H. *et al.* (2012) Silver nanorice structures: oriented attachment-dominated growth, high environmental sensitivity, and real-space visualization of multipolar resonances. *Chem. Mater.* 24, 2339-2346
- [31] Jung, H. et al. (2015) Bridging the nanogap with light: continuous tuning of plasmon coupling between gold nanoparticles. ACS nano 9, 12292-12300
- [32] Wang, H. et al. (2007) Plasmonic nanostructures: artificial molecules. Acc. Chem. Res. 40, 53-62
- [33] Jain, P. K. *et al.* (2007) Review of some interesting surface plasmon resonance-enhanced properties of noble metal nanoparticles and their applications to biosystems. *Plasmonics* 2, 107-118
- [34] Pelton, M. et al. (2008) Metal nanoparticle plasmonics. Laser Photonics Rev. 2, 136-159
- [35] Rycenga, M. *et al.* (2011) Controlling the synthesis and assembly of silver nanostructures for plasmonic applications. *Chem. Rev.* 111, 3669-3712
- [36] Halas, N. J. et al. (2011) Plasmons in strongly coupled metallic nanostructures. *Chem. Rev.* 111, 3913-3961
- [37] Jones, M. R. *et al.* (2011) Templated techniques for the synthesis and assembly of plasmonic nanostructures. *Chem. Rev.* 111, 3736-3827
- [38] Klinkova, A. et al. (2014) Self-assembled plasmonic nanostructures. *Chem. Soc. Rev.* 43, 3976-3991
- [39] Li, J.-F. et al. (2017) Plasmon-enhanced fluorescence spectroscopy. Chem. Soc. Rev. 46, 3962-3979
- [40] Wu, X. et al. (2018) Environmentally responsive plasmonic nanoassemblies for biosensing. *Chem. Soc. Rev.* 47, 4677-4696
- [41] Lu, D. et al. (2019) Self Assembly of Polymer Coated Plasmonic Nanocrystals: From Synthetic Approaches to Practical Applications. *Macromol. Rapid Commun.* 40, 1800613
- [42] Clavero, C. (2014) Plasmon-induced hot-electron generation at nanoparticle/metal-oxide interfaces for photovoltaic and photocatalytic devices. *Nature Photon.* 8, 95
- [43] Wakeham, D. et al. (2009) Influence of temperature and molecular structure on ionic liquid solvation layers. J. Phys. Chem. B 113, 5961-5966
- [44] He, L. *et al.* (2012) Determination of solvation layer thickness by a magnetophotonic approach. *ACS nano* 6, 4196-4202
- [45] Xu, W. et al. (2018) Colloidal Assembly Approaches to Micro/Nanostructures of Complex Morphologies. *Small* 14, 1801083
- [46] Zhang, H.and Wang, D. (2008) Controlling the growth of charged nanoparticle chains through interparticle electrostatic repulsion. *Angew. Chem. Int. Ed.* 47, 3984-3987
- [47] Lin, S. *et al.* (2005) One dimensional plasmon coupling by facile self assembly of gold nanoparticles into branched chain networks. *Adv. Mater.* 17, 2553-2559
- [48] Bishop, K. J. et al. (2009) Nanoscale forces and their uses in self assembly. small 5, 1600-1630
- [49] Wang, J.-C. *et al.* (2006) On one-dimensional self-assembly of surfactant-coated nanoparticles. *J. Chem. Phys.* 125, 194717

- [50] Chen, Q. et al. (2011) Supracolloidal reaction kinetics of Janus spheres. Science 331, 199-202
- [51] Cheng, L. *et al.* (2010) Responsive plasmonic assemblies of amphiphilic nanocrystals at oilwater interfaces. *Acs Nano* 4, 6098-6104
- [52] Sun, Z. et al. (2008) pH controlled reversible assembly and disassembly of gold nanorods. small 4, 1287-1292
- [53] Song, J. *et al.* (2011) Plasmonic vesicles of amphiphilic gold nanocrystals: self-assembly and external-stimuli-triggered destruction. *J. Am. Chem. Soc.* 133, 10760-10763
- [54] Zhang, Z. et al. (2013) Salt plays a pivotal role in the temperature-responsive aggregation and layer-by-layer assembly of polymer-decorated gold nanoparticles. *Chem. Mater.* 25, 4297-4303
- [55] Zhang, H. *et al.* (2017) Interfacial Self-Assembly of Polyelectrolyte-Capped Gold Nanoparticles. *Langmuir* 33, 12227-12234
- [56] Shen, Y. *et al.* (2008) Gold nanoparticles coated with a thermosensitive hyperbranched polyelectrolyte: towards smart temperature and pH nanosensors. *Angew. Chem. Int. Ed.* 47, 2227-2230
- [57] Zhang, X. et al. (2016) Self-assembly of one-dimensional nanocrystal superlattice chains mediated by molecular clusters. J. Am. Chem. Soc. 138, 3290-3293
- [58] Wang, H. et al. (2012) Unconventional Chain Growth Mode in the Assembly of Colloidal Gold Nanoparticles. *Angew. Chem. Int. Ed.* 51, 8021-8025
- [59] Vogele, K. *et al.* (2016) Self-assembled active plasmonic waveguide with a peptide-based thermomechanical switch. *ACS nano* 10, 11377-11384
- [60] Leung, F. C.-M. *et al.* (2016) Metal–metal and  $\pi$ – $\pi$  interactions directed end-to-end assembly of gold nanorods. *J. Am. Chem. Soc.* 138, 2989-2992
- [61] Wang, Y. et al. (2010) End-to-end assembly of gold nanorods by means of oligonucleotide—mercury (II) molecular recognition. Chem. Commun. 46, 1332-1334
- [62] Bhattacharjee, S. *et al.* (1998) DLVO interaction between colloidal particles: beyond Derjaguin's approximation. *Croat. Chem. Acta* 71, 883-903
- [63] Yin, Y.and Alivisatos, A. P. (2005) Colloidal nanocrystal synthesis and the organic–inorganic interface. *Nature* 437, 664-670
- [64] Batista, C. A. S. et al. (2015) Nonadditivity of nanoparticle interactions. Science 350, 1242477
- [65] Liu, K. et al. (2010) Step-growth polymerization of inorganic nanoparticles. Science 329, 197-200
- [66] Wang, X. et al. (2008) Polymer-encapsulated gold-nanoparticle dimers: facile preparation and catalytical application in guided growth of dimeric ZnO-nanowires. *Nano Lett.* 8, 2643-2647
- [67] Liu, K. et al. (2014) Copolymerization of metal nanoparticles: a route to colloidal plasmonic copolymers. *Angew. Chem. Int. Ed.* 53, 2648-2653
- [68] Yi, C. et al. (2019) Alternating Copolymerization of Inorganic Nanoparticles. J. Am. Chem. Soc.
- [69] Shah, A. A. *et al.* (2015) Actuation of shape-memory colloidal fibres of Janus ellipsoids. *Nature Mater.* 14, 117
- [70] Gröschel, A. H. *et al.* (2013) Guided hierarchical co-assembly of soft patchy nanoparticles. *Nature* 503, 247
- [71] Zhuang, Z. et al. (2016) Hierarchical nanowires synthesized by supramolecular stepwise polymerization. *Angew. Chem.* 128, 12710-12715
- [72] Cheng, X. *et al.* (2018) Controllable oligomerization: defying step-growth kinetics in the polymerization of gold nanoparticles. *Chem. Commun.* 54, 7746-7749
- [73] Yi, C. *et al.* (2019) Alternating Copolymerization of Inorganic Nanoparticles. *J. Am. Chem. Soc.* 141, 7917-7925
- [74] Klinkova, A. *et al.* (2013) Colloidal analogs of molecular chain stoppers. *Proc. Natl. Acad. Sci. U.S.A.* 110, 18775-18779
- [75] Romo-Herrera, J. M. *et al.* (2011) Controlled assembly of plasmonic colloidal nanoparticle clusters. *Nanoscale* 3, 1304-1315

- [76] Prodan, E. *et al.* (2003) A hybridization model for the plasmon response of complex nanostructures. *Science* 302, 419-422
- [77] Nordlander, P. et al. (2004) Plasmon hybridization in nanoparticle dimers. Nano Lett. 4, 899-903
- [78] Prodan, E.and Nordlander, P. (2004) Plasmon hybridization in spherical nanoparticles. *J. Chem. Phys.* 120, 5444-5454
- [79] Yang, S.-C. *et al.* (2010) Plasmon hybridization in individual gold nanocrystal dimers: direct observation of bright and dark modes. *Nano Lett.* 10, 632-637
- [80] Atay, T. *et al.* (2004) Strongly interacting plasmon nanoparticle pairs: from dipole dipole interaction to conductively coupled regime. *Nano Lett.* 4, 1627-1631
- [81] Rechberger, W. *et al.* (2003) Optical properties of two interacting gold nanoparticles. *Opt. Commun.* 220, 137-141
- [82] Zhang, T. *et al.* (2014) Unconventional route to encapsulated ultrasmall gold nanoparticles for high-temperature catalysis. *ACS nano* 8, 7297-7304
- [83] Gao, C. et al. (2012) One-step seeded growth of Au nanoparticles with widely tunable sizes. Nanoscale 4, 2875-2878
- [84] Liu, X. et al. (2013) Size-tailored synthesis of silver quasi-nanospheres by kinetically controlled seeded growth. *Langmuir* 29, 10559-10565
- [85] Li, M. et al. (2011) A Generalized Mechanism for Ligand Induced Dipolar Assembly of Plasmonic Gold Nanoparticle Chain Networks. Adv. Funct. Mater. 21, 851-859
- [86] Hill, L. J. *et al.* (2015) Colloidal polymers from inorganic nanoparticle monomers. *Prog. Polym. Sci.* 40, 85-120
- [87] Tan, S. J. et al. (2011) Building plasmonic nanostructures with DNA. Nat. Nanotechnol. 6, 268
- [88] Kotov, N. *et al.* (1994) Monoparticulate layer and Langmuir-Blodgett-type multiparticulate layers of size-quantized cadmium sulfide clusters: A colloid-chemical approach to superlattice construction. *J. Phys. Chem.* 98, 2735-2738
- [89] Murray, C. B. *et al.* (2000) Synthesis and characterization of monodisperse nanocrystals and close-packed nanocrystal assemblies. *Annu. Rev. Mater. Sci.* 30, 545-610
- [90] Sastry, M. *et al.* (1998) Optical Absorption Study of the Biotin– Avidin Interaction on Colloidal Silver and Gold Particles. *Langmuir* 14, 4138-4142
- [91] Han, X. et al. (2011) Role of salt in the spontaneous assembly of charged gold nanoparticles in ethanol. *Langmuir* 27, 5282-5289
- [92] Pramod, P.and Thomas, K. G. (2008) Plasmon coupling in dimers of Au nanorods. *Adv. Mater.* 20, 4300-4305
- [93] Tang, Z.and Kotov, N. A. (2005) One dimensional assemblies of nanoparticles: preparation, properties, and promise. *Adv. Mater.* 17, 951-962
- [94] Coomber, D. *et al.* (2010) Programmed assembly of peptide-functionalized gold nanoparticles on DNA templates. *Langmuir* 26, 13760-13762
- [95] Wang, Y. et al. (2010) A systems approach towards the stoichiometry-controlled hetero-assembly of nanoparticles. *Nat. Commun.* 1, 87
- [96] Butt, H.-J. et al., Physics and chemistry of interfaces, John Wiley & Sons, 2013.
- [97] Gao, C. et al. (2014) Fully alloyed Ag/Au nanospheres: combining the plasmonic property of Ag with the stability of Au. J. Am. Chem. Soc. 136, 7474-7479
- [98] López Lozano, X. c. et al. (2013) Effect of alloying on the optical properties of Ag–Au nanoparticles. J. Phys. Chem. C 117, 3062-3068
- [99] Narayanaswamy, A. *et al.* (2006) Crystalline nanoflowers with different chemical compositions and physical properties grown by limited ligand protection. *Angew. Chem. Int. Ed.* 45, 5361-5364

- [100] Narayanaswamy, A. *et al.* (2006) Formation of nearly monodisperse In2O3 nanodots and oriented-attached nanoflowers: hydrolysis and alcoholysis vs pyrolysis. *J. Am. Chem. Soc.* 128, 10310-10319
- [101] Liu, L. et al. (2018) Reversible assembly and dynamic plasmonic tuning of Ag nanoparticles enabled by limited ligand protection. *Nano Lett.* 18, 5312-5318
- [102] Zhang, L. et al. (1996) Ion-induced morphological changes in "crew-cut" aggregates of amphiphilic block copolymers. *Science* 272, 1777-1779
- [103] Liu, C. et al. (2011) Toroidal Micelles of Polystyrene block Poly (acrylic acid). Small 7, 2721-2726
- [104] Yang, M. et al. (2010) Mechanistic investigation into the spontaneous linear assembly of gold nanospheres. *PCCP* 12, 11850-11860
- [105] Chen, Q. *et al.* (2015) Interaction potentials of anisotropic nanocrystals from the trajectory sampling of particle motion using in situ liquid phase transmission electron microscopy. *ACS Cent. Sci.* 1, 33-39
- [106] Nie, Z. et al. (2007) Self-assembly of metal—polymer analogues of amphiphilic triblock copolymers. *Nature Mater.* 6, 609
- [107] Zhang, Y. et al. (2015) Metal nanoparticle dispersion, alignment, and assembly in nematic liquid crystals for applications in switchable plasmonic color filters and E-polarizers. Acs Nano 9, 3097-3108
- [108] Kristensen, A. et al. (2016) Plasmonic colour generation. Nat. Rev. Mater. 2, 1-14
- [109] Wang, L. et al. (2010) Side by side and end to end gold nanorod assemblies for environmental toxin sensing. Angew. Chem. Int. Ed. 49, 5472-5475
- [110] Malinsky, M. D. *et al.* (2001) Chain length dependence and sensing capabilities of the localized surface plasmon resonance of silver nanoparticles chemically modified with alkanethiol self-assembled monolayers. *J. Am. Chem. Soc.* 123, 1471-1482
- [111] Liu, B. *et al.* (2018) pH and Temperature Dual-Responsive Plasmonic Switches of Gold Nanoparticle Monolayer Film for Multiple Anticounterfeiting. *Langmuir* 34, 13047-13056
- [112] Liu, L. et al. (2019) Dynamic color switching of plasmonic nanoparticle films. *Angew. Chem.* 131, 16453-16459
- [113] Le Ru, E.and Etchegoin, P. (2006) Rigorous justification of the | E | 4 enhancement factor in surface enhanced Raman spectroscopy. *Chem. Phys. Lett.* 423, 63-66
- [114] Qian, X. et al. (2009) Stimuli-responsive SERS nanoparticles: conformational control of plasmonic coupling and surface Raman enhancement. J. Am. Chem. Soc. 131, 7540-7541
- [115] Guerrini, L. *et al.* (2012) Tuning the interparticle distance in nanoparticle assemblies in suspension via DNA-triplex formation: correlation between plasmonic and surface-enhanced Raman scattering responses. *Chem. Sci.* 3, 2262-2269
- [116] Dasary, S. S. *et al.* (2009) Gold nanoparticle based label-free SERS probe for ultrasensitive and selective detection of trinitrotoluene. *J. Am. Chem. Soc.* 131, 13806-13812
- [117] Zhu, Z. et al. (2018) Plasmon-enhanced fluorescence in coupled nanostructures and applications in DNA detection. ACS Applied Bio Materials 1, 118-124
- [118] Chen, Y.-S. *et al.* (2017) Dynamic contrast-enhanced photoacoustic imaging using photothermal stimuli-responsive composite nanomodulators. *Nat. Commun.* 8, 1-10
- [119] Schild, H. G. (1992) Poly (N-isopropylacrylamide): experiment, theory and application. *Prog. Polym. Sci.* 17, 163-249
- [120] Tang, F. *et al.* (2012) Control of metal-enhanced fluorescence with pH-and thermoresponsive hybrid microgels. *Langmuir* 28, 883-888
- [121] Li, Z. et al. (2019) Magnetic Assembly of Nanocubes for Orientation-Dependent Photonic Responses. *Nano Lett.* 19, 6673-6680

[122] Myroshnychenko, V. *et al.* (2008) Modelling the optical response of gold nanoparticles. *Chem. Soc. Rev.* 37, 1792-1805

[123] Ding, S.-Y. et al. (2016) Nanostructure-based plasmon-enhanced Raman spectroscopy for surface analysis of materials. *Nat. Rev. Mater.* 1, 16021

# **Glossary**

**Electrical double layer**: a two parallel layer of charges that appears on the surface of colloidal particles in a colloidal dispersion and is responsible for the colloidal stability and interparticle interactions.

**Entropic forces**: the interactions between particles in colloidal dispersions due to the osmotic pressure that arises from particle crowding, which are often responsible for driving the self-assembly of colloidal particles.

**Localized surface plasmon resonance (LSPR)**: the resonance of the coherent electron oscillation localized at the surface of conductive particles, which is produced through the electromagnetic interaction of the particle with incident light of a specific frequency (resonant frequency).

**Nonadditivity**: the features of the nonadditive potential of interacting nanoparticles due to the discreteness and fluctuations of matter when two nanoparticles approach a distance smaller than several tens of nanometers.

**Plasmon band**: a specific energy level where the LSPR occurs.

**Solution-processed assembly**: the assembly of nanoparticles that occurs in a solution phase.

**Surface-enhanced Raman spectroscopy (SERS)**: a surface-sensitive phenomenon that remarkably enhances Raman scattering of molecules usually absorbed on the surface of plasmonic colloids.

Van der Waals (vdW) force: a distance-dependent interaction between atoms or molecules originating from correlations in the fluctuating polarizations of neighboring atoms or molecules, which includes Keesom force (the electrostatic interactions between permanent charges or multipoles), Debye force (the attractive interaction between a permanent multipole with an induced multipole), and London dispersion interactions (the attractive interaction between any pair instantaneous multipoles).

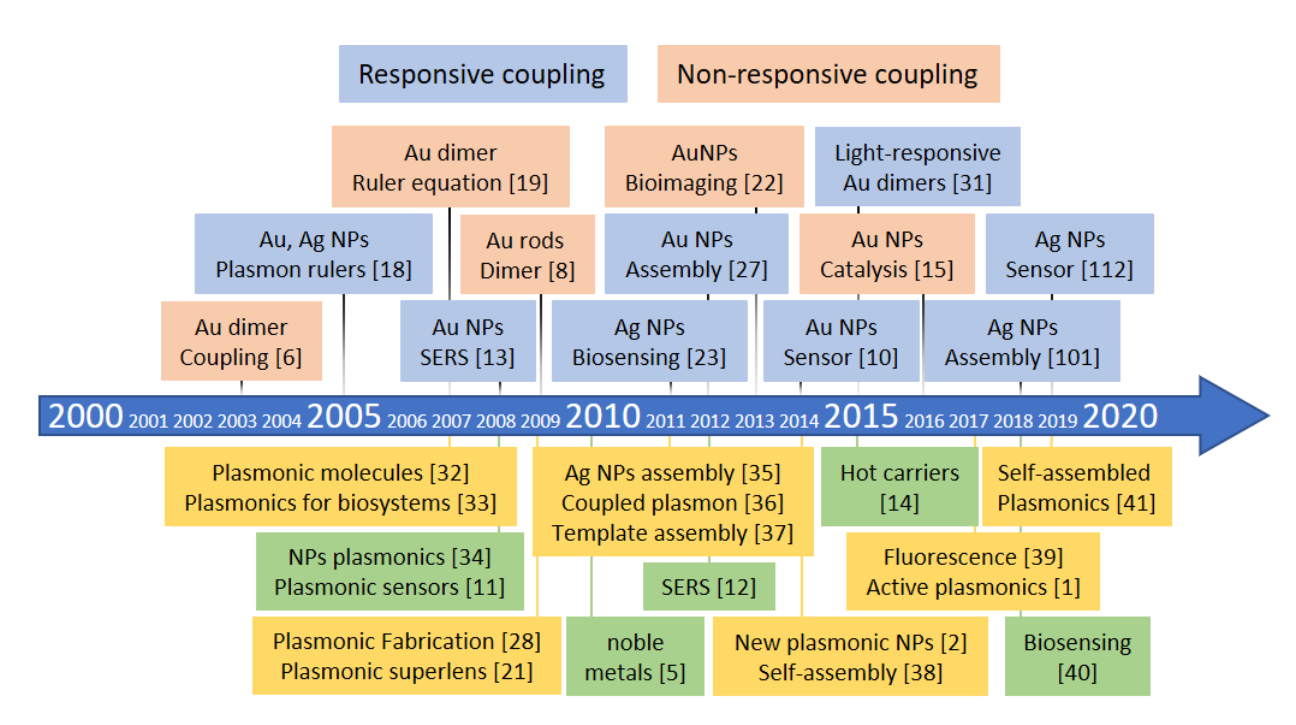


**Figure 1**. Timeline showing key developments (top panel) and representative reviews (bottom panel) in the assembly of plasmonic nanostructures. NPs: nanoparticles.

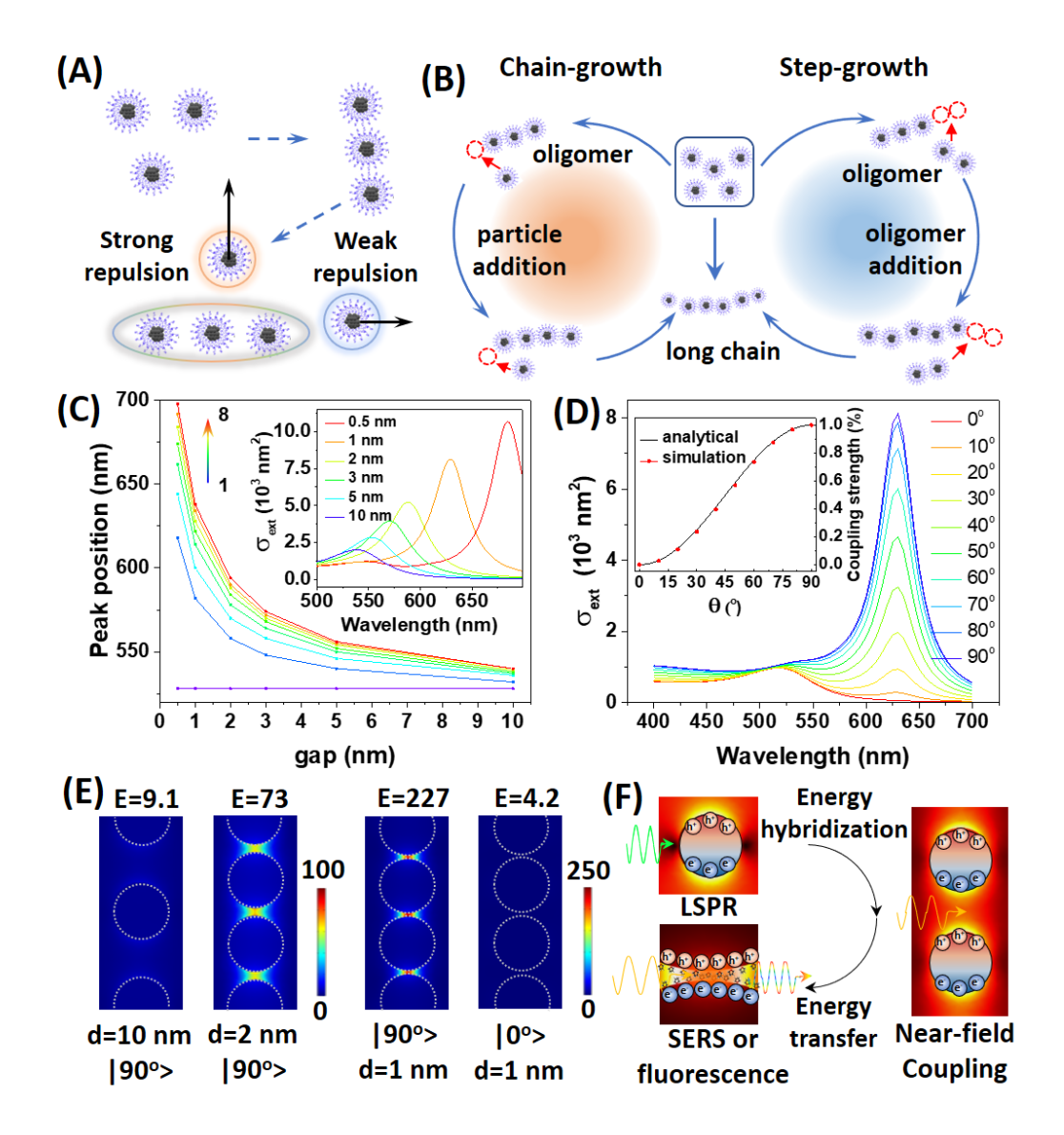


**Figure 2.** General concepts of plasmon coupling in the colloidal self-assembly of plasmonic nanospheres. (A) Assembly mechanism of anisotropic plasmonic chains. (B) Assembly pathway: chain-growth versus step-growth polymerization. (C) Theoretical analysis of the peak position of plasmonic chains. Inset: calculated extinction cross-section of plasmonic chains of six Au nanoparticles with different separation. (D) Calculated extinction cross-section of plasmonic chains under different orientations. Data source: finite-element-analysis of plasmonic excitation of linear Au chains at a fixed separation (1 nm). Inset: the correlation between coupling strength and orientation predicted from simulation and analytical analysis. The coupling strength is 100% and 0% when the peak intensity is highest and lowest, respectively. (E) Finite-element solutions

of enhanced electric fields. In theoretical consideration, d is the gap size of six Au nanoparticles (15 nm in diameter) in a linear chain. The left two panels show the gap size-dependent plasmon coupling while the right two panels show the orientation-dependent plasmon coupling. (F) Illustration of the energy hybridization in plasmonic coupling and the energy transfer for enhanced spectroscopy.

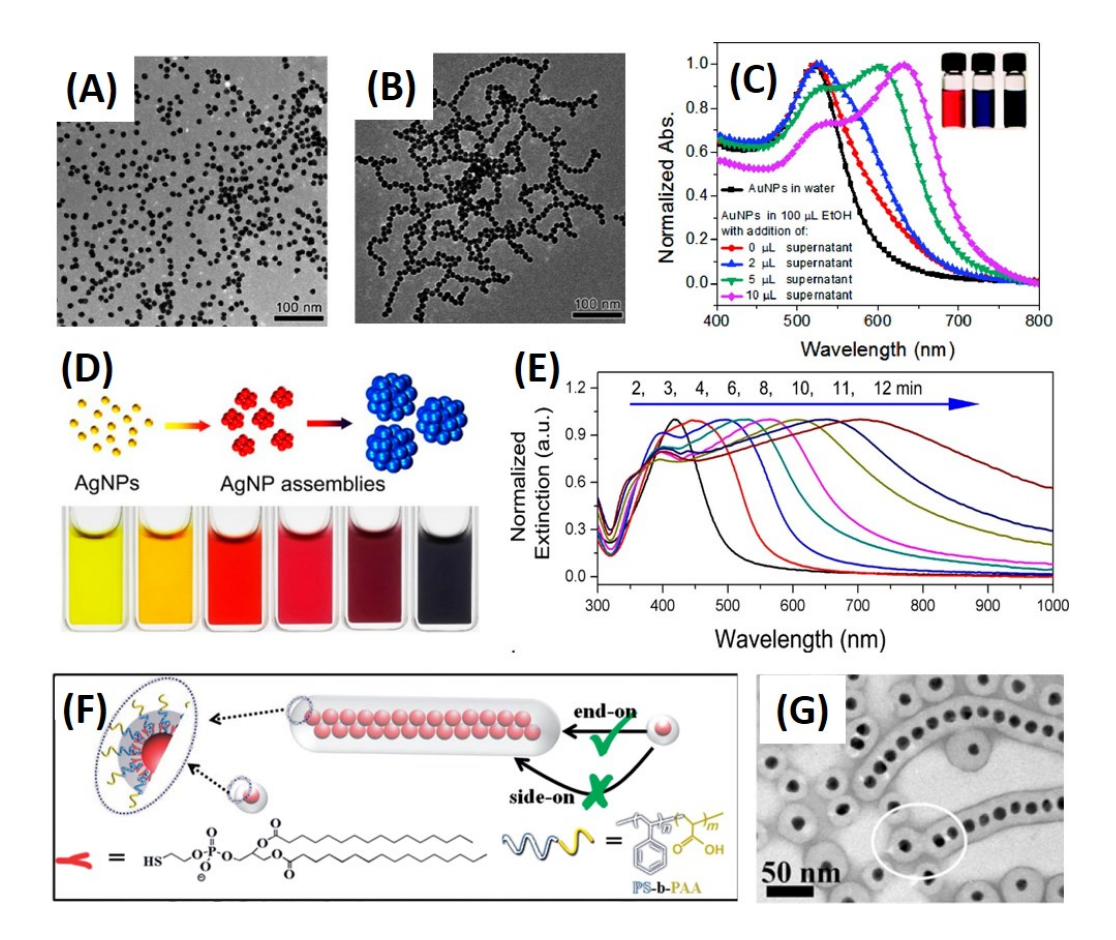


**Figure 3**. Assembly pathways of colloidal plasmonic nanospheres. Transmission electron microscopy (TEM) images of (A) monodisperse Au nanoparticles and (B) branched chains after assembly. (C) Normalized UV-vis extinction spectra of Au nanoparticles in ethanol with the addition of different salts. Insets: digital images of AuNRs dispersions during the assembly process. Adapted from [91]. (D) Digital photographs of Ag nanoparticles and assemblies obtained with different reaction times. (E) Extinction spectra the of the plasmon bands during assembly. Adapted from [101]. (F) Schematics illustration of the 1D assembly of Au nanoparticles through the chain-growth pathway. (G) TEM image of the intermediate species during chain growth in assembly. Adapted from [58].

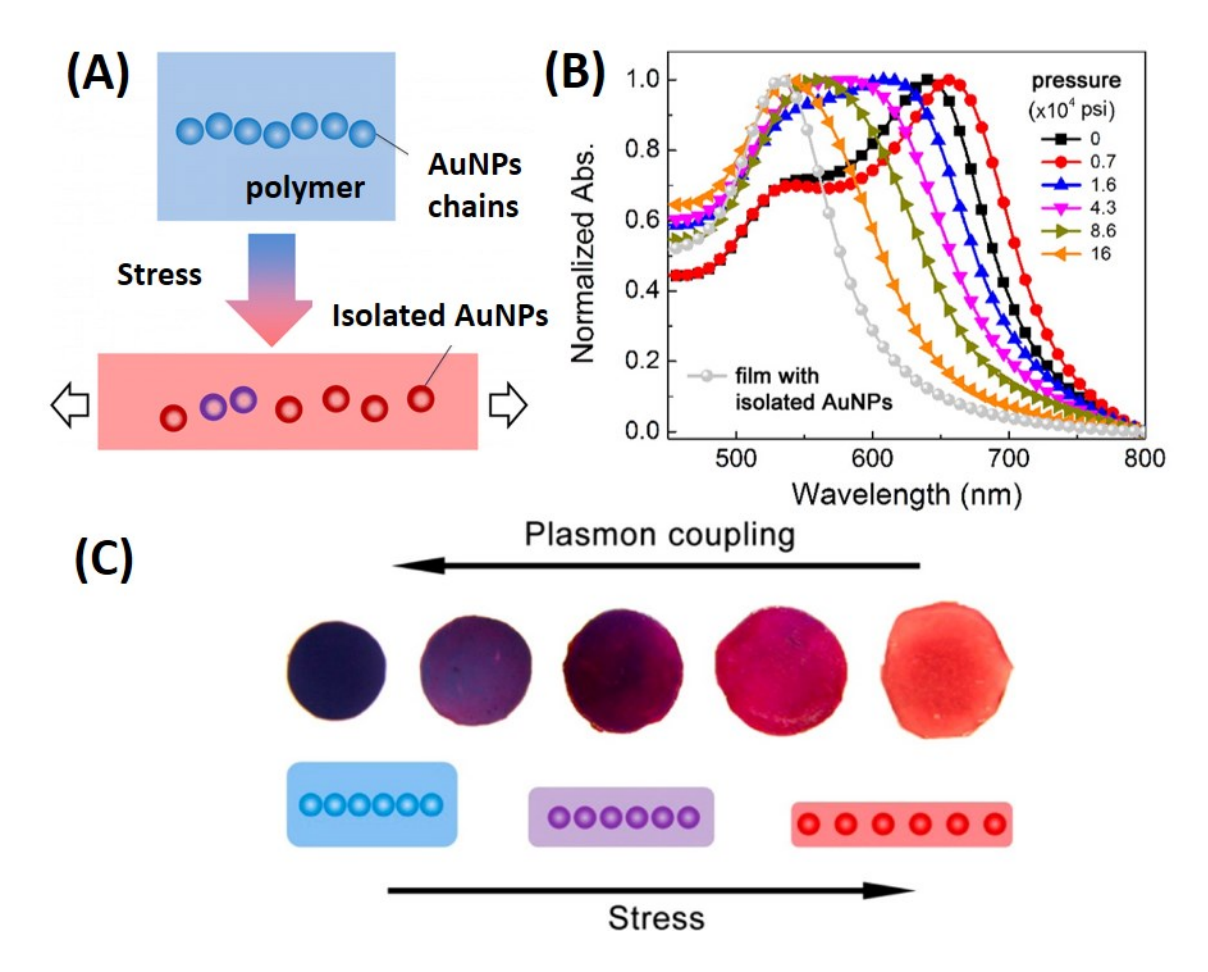


**Figure 4**. Colorimetric stress sensor based on plasmon coupling. (A) Schematic illustration of the colorimetric film based on disassembly of Au nanoparticles chains. (B) The UV-vis extinction spectra of the composite film after different pressures. (C) Digital images of films after experiencing different pressures [10].

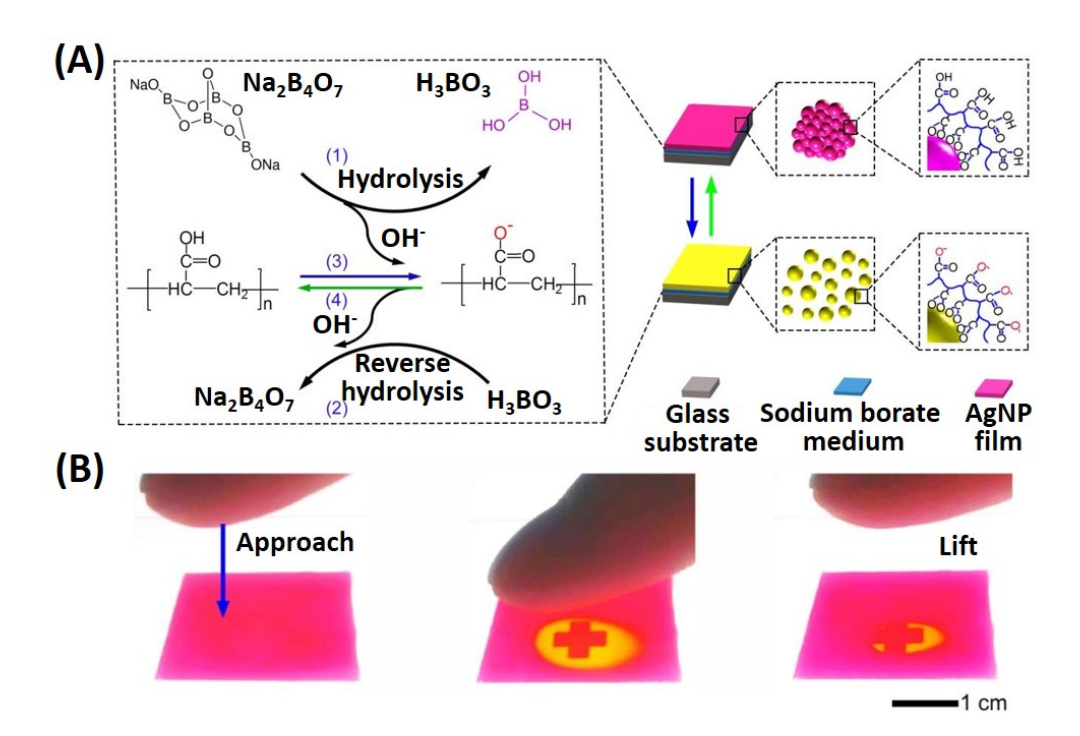


**Figure 5**. Dynamic color-switching based on reversible plasmon coupling. (A) Design of the plasmonic color-switchable Ag nanoparticles film. (B) Digital photographs showing the touchless fingertip activated encryption and decryption process of the encrypted Ag nanoparticles film [112].

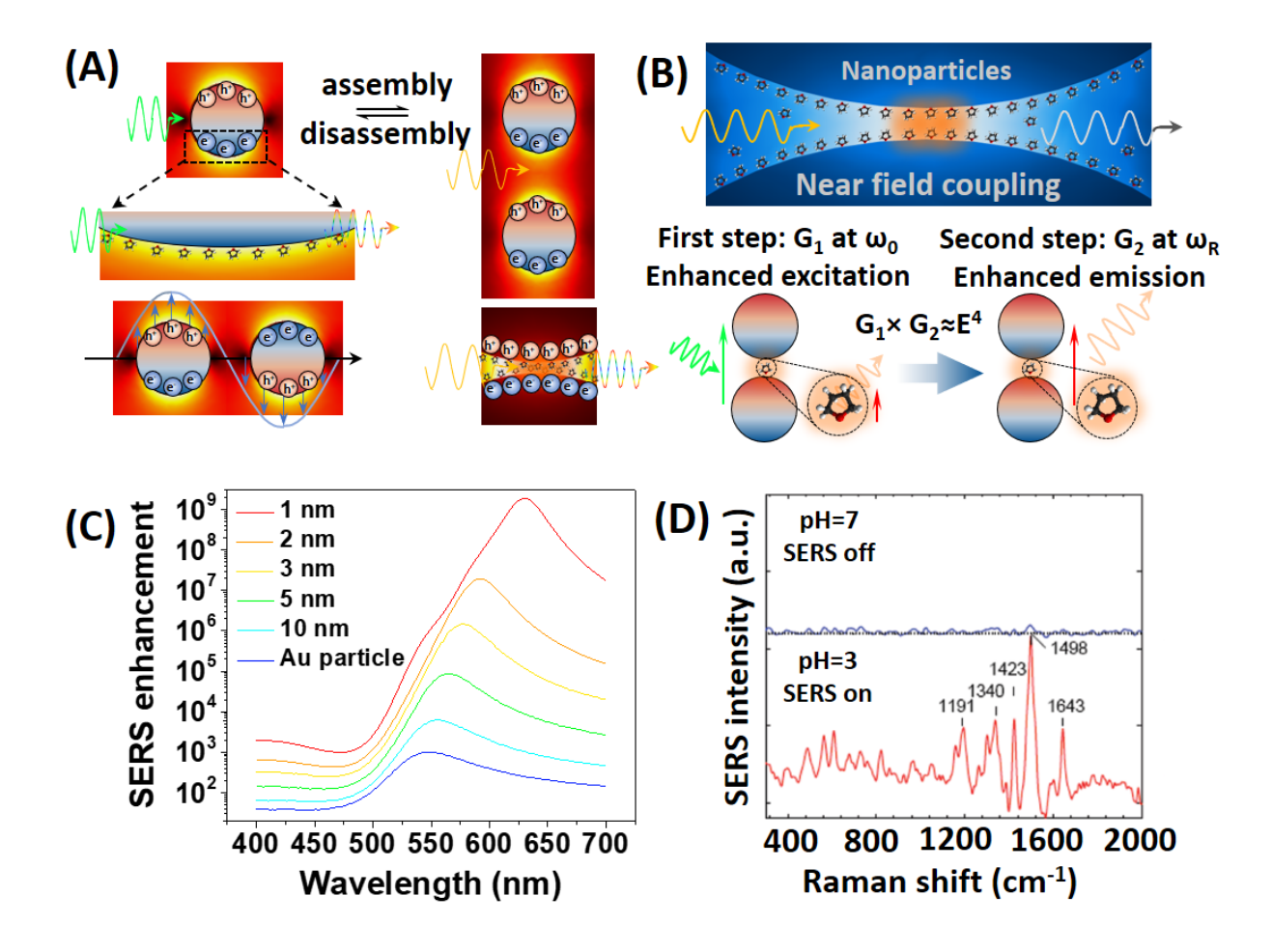


**Figure 6**. Plasmon coupling for surface-enhanced spectroscopy. (A) Plasmon coupling promotes the performance of enhanced spectroscopy. (B) Schematic illustration of plasmon coupling-enhanced emission from Raman and fluorescent molecules. Adapted from [123]. (C) Theoretical SERS enhancement calculated by finite element analysis. A plasmonic chain of Au nanoparticles with a diameter of 15 nm is considered for this plot. (D) Reversible activation of SERS in response to pH changes [114].